Supporting Information

Assessing the impact of antisolvent-regulated $ZnCl_2$ water-in-salt electrolyte on solvation structure: a multiscale computational validation for aqueous Zn-ion battery application

Asis Sethi,[1,2] Chaithra Rajeev,[1] Anil Kumar U.,[1,2] Parul Sharma,[3] Anurag Prakash Sunda,[3]* and Vishal M. Dhavale[1,2]*

[1] CSIR-Central Electrochemical Research Institute, CSIR Madras Complex, Taramani, Chennai 600 113, Tamil Nadu, India

[2] Academy of Scientific and Innovative Research (AcSIR), Ghaziabad- 201002, India
*Email: vishal@cecri.res.in

[3] Department of Chemistry, J. C. Bose University of Science and Technology, YMCA, Faridabad 121006, India
*Email: anurag@jcboseust.ac.in; anurag.sunda@gmail.com

Table of Contents

Section S1: Solubility test

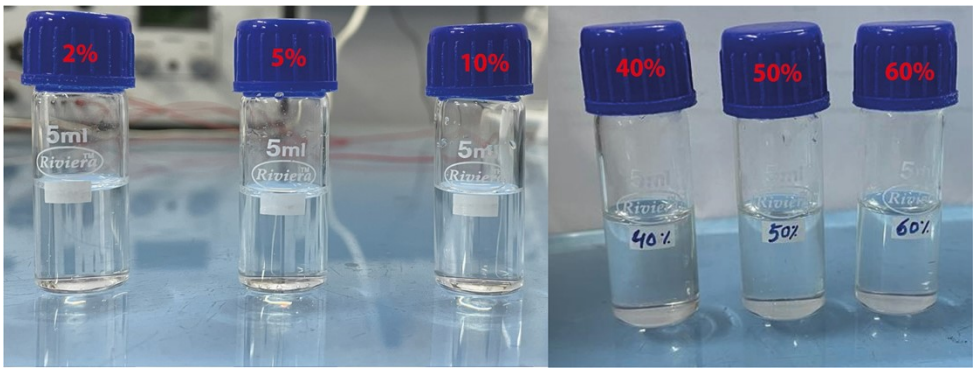

Fig. S1: *Solubility test of different vol.% of methanol in 10 m $ZnCl_2$-WiSE. It depicts 10 m $ZnCl_2$ -WiSE and methanol forming a homogeneous solution without precipitation or delamination.*

Section S2: Raman and Infrared Spectroscopy

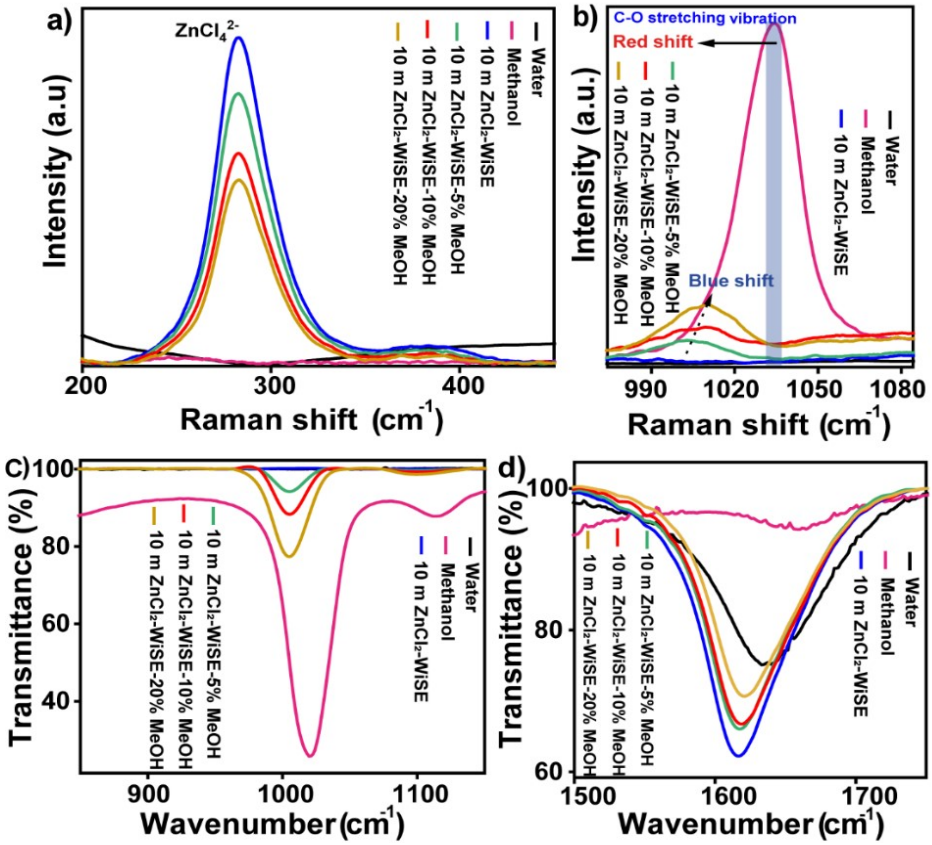

Fig. S2: *(a &b) Raman spectra, and (c & d) FT-IR spectra of water, methanol, 10 m $ZnCl_2$-WiSE, 10 m-$ZnCl_2$-WiSE-x% MeOH (x= 5, 10, 20) showing $ZnCl_4^{2-}$ and C-O bond Raman shift peak, C-O bond stretching peak, O-H bond bending peak, respectively.*

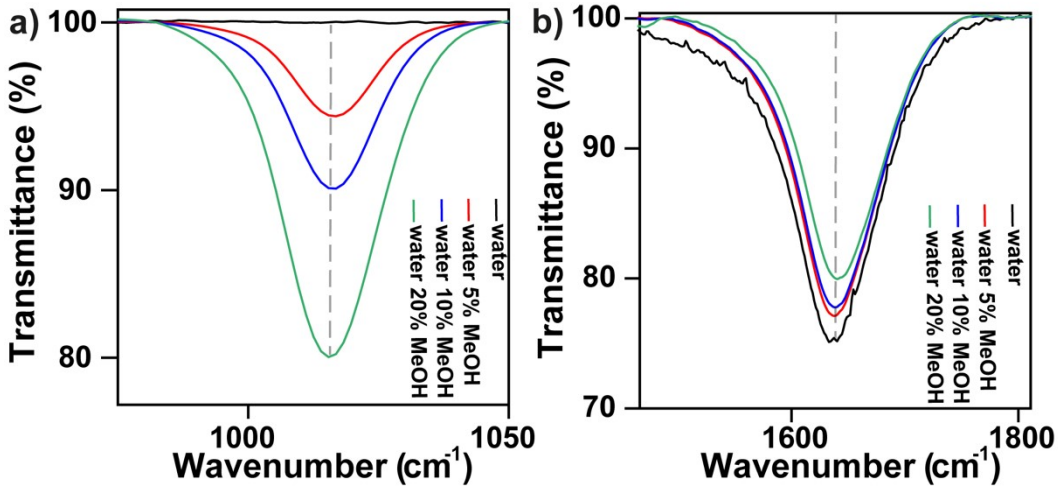

***Fig. S3**: FT-IR spectra of a mixture of pure water and different vol.% of pure methanol (a) C-O bond stretching, and (b) O-H bond bending vibration.*

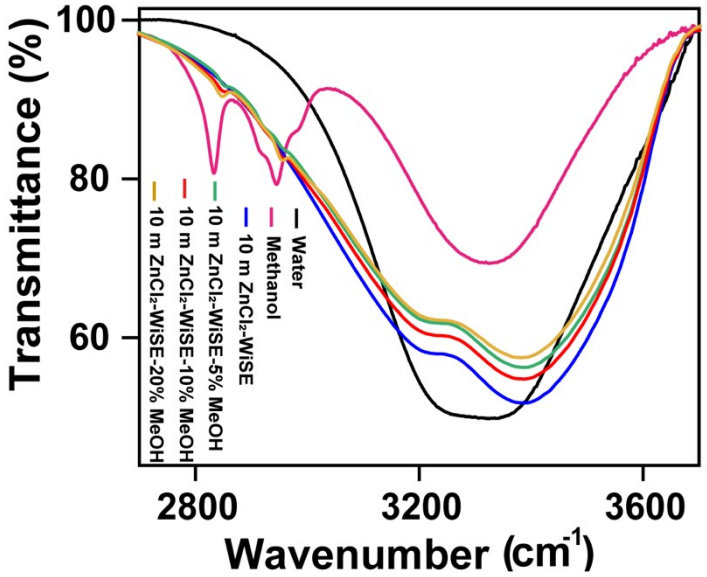

***Fig. S4**: FT-IR spectra of water, methanol, 10 m $ZnCl_2$-WiSE and 10 m $ZnCl_2$-WiSE-x % MeOH show the O-H bond stretching vibration shift.*

Section S3: Spatial Distribution Function Calculation

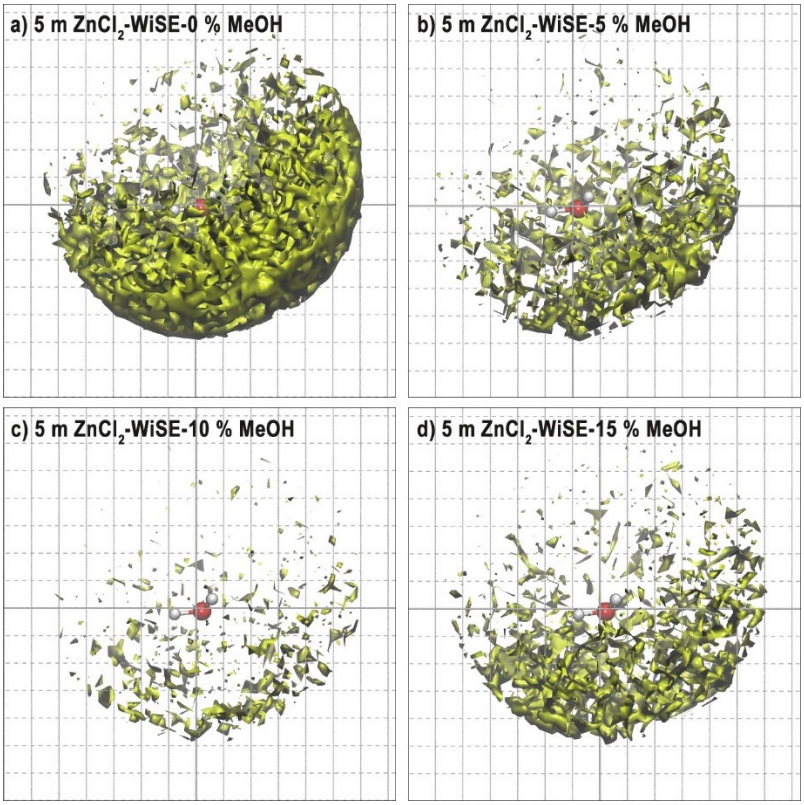

Fig. S5: *Spatial distribution function (SDF) calculated from MD simulations to depict water-zinc interactions for 5 m $ZnCl_2$-WiSE-x % MeOH with (a) x=0, (b) x=5, (c) x=10, and (d) x=15 [Colour scheme: H_2O (Ball and Stick) H-White, O-Red; Zinc Ions (Isosurface)-Yellow-green (Iso value: 0.0032 Å^3)].*

Section S4: X-Ray Diffraction

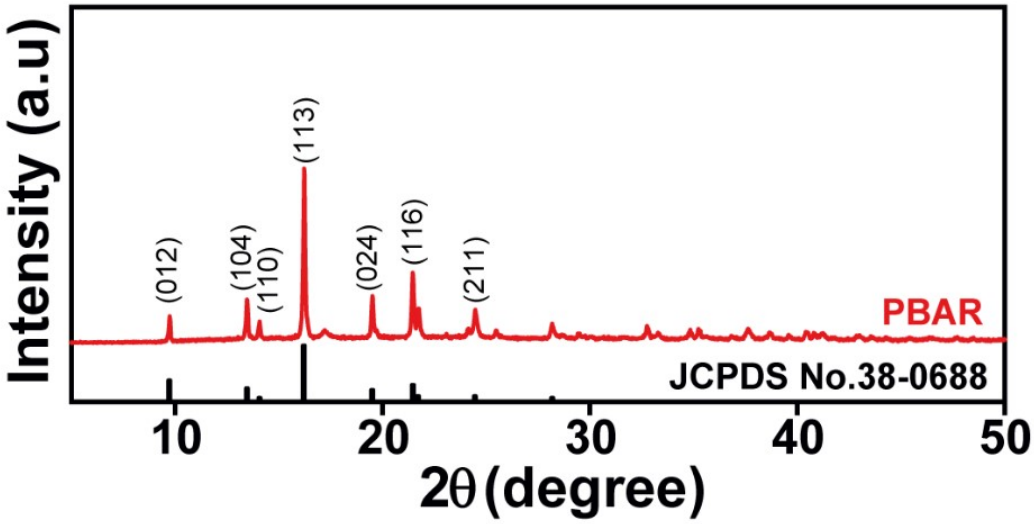

Fig. S6: *Powder-XRD pattern of PBAR. The peaks are indexed to its JCPDS Card. No. 38-0688.*

Section S5: Field-Emission Scanning Electron Microscopy (FE-SEM)

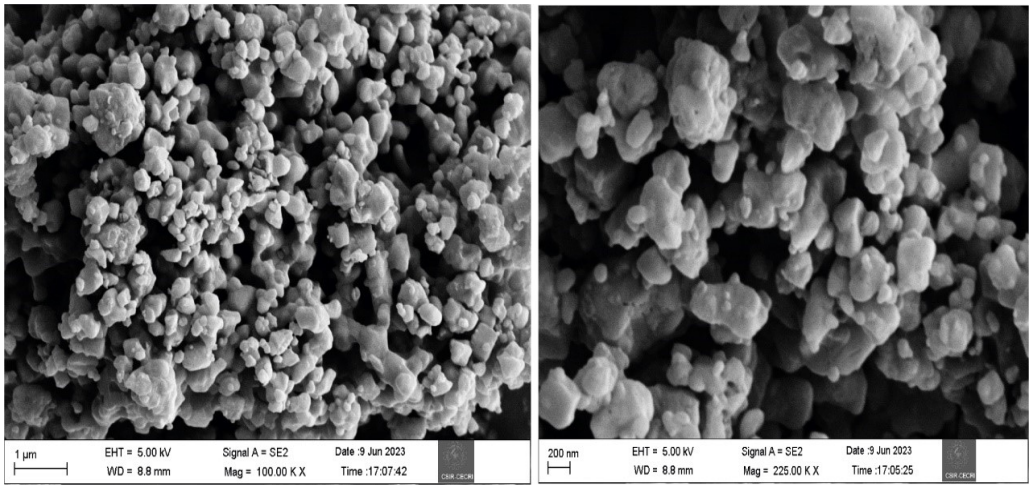

Fig. S7: *Field emission scanning electron microscopy (FE-SEM) images of PBAR recorded at different magnifications.*

Section S6: Electrochemical Characterization

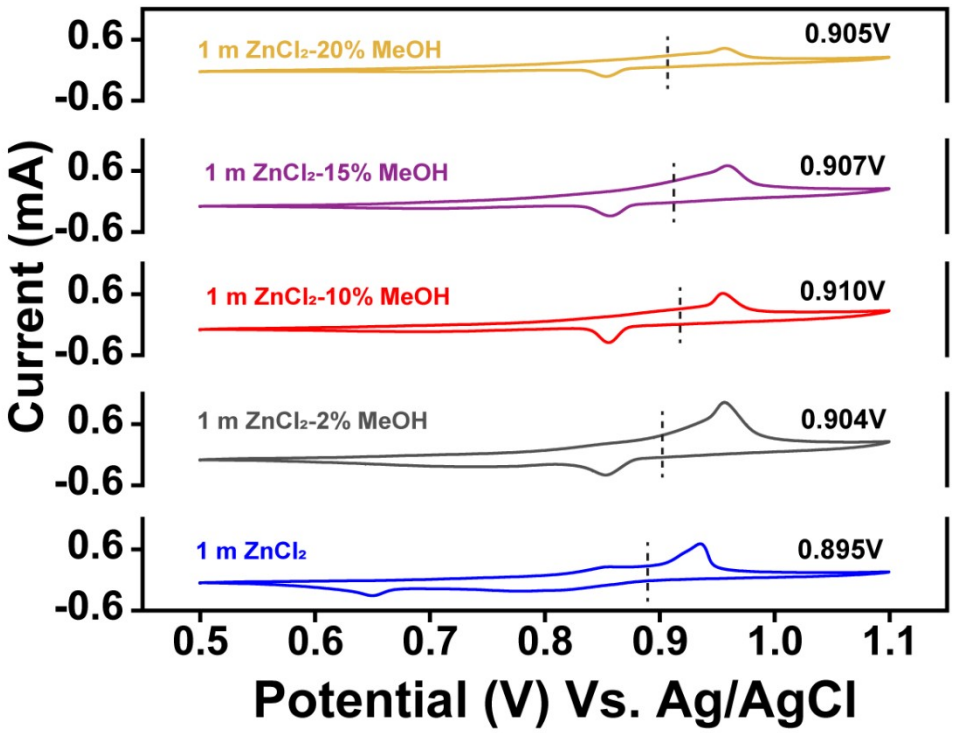

Fig. S8: *Comparative cyclic voltammogram of PBAR in different vol.% of methanol added into 1m $ZnCl_2$ aqueous electrolyte (1 mZA). It shows that in 10 vol.% methanol addition, the redox potential is highest, 0.910 V vs Ag/AgCl.*

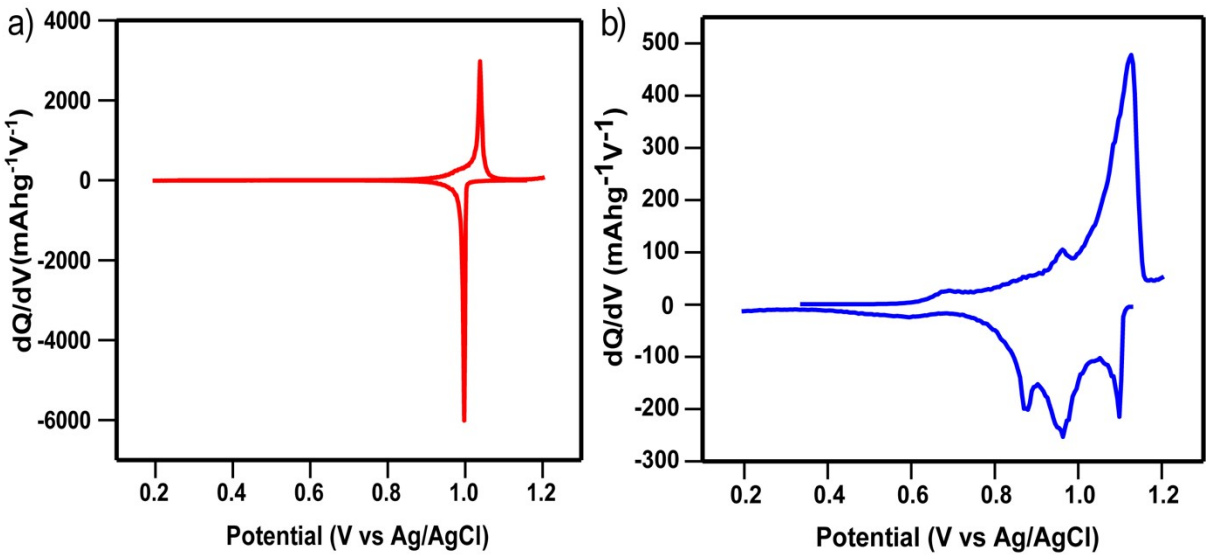

Fig. S9: *Derivative plot of PBAR charge-discharge curve in a) 10 m $ZnCl_2$-WiSE-10 % MeOH, and b) 10 m $ZnCl_2$-WiSE.*

Section S7: Electrochemical Impedance Spectroscopy (EIS)

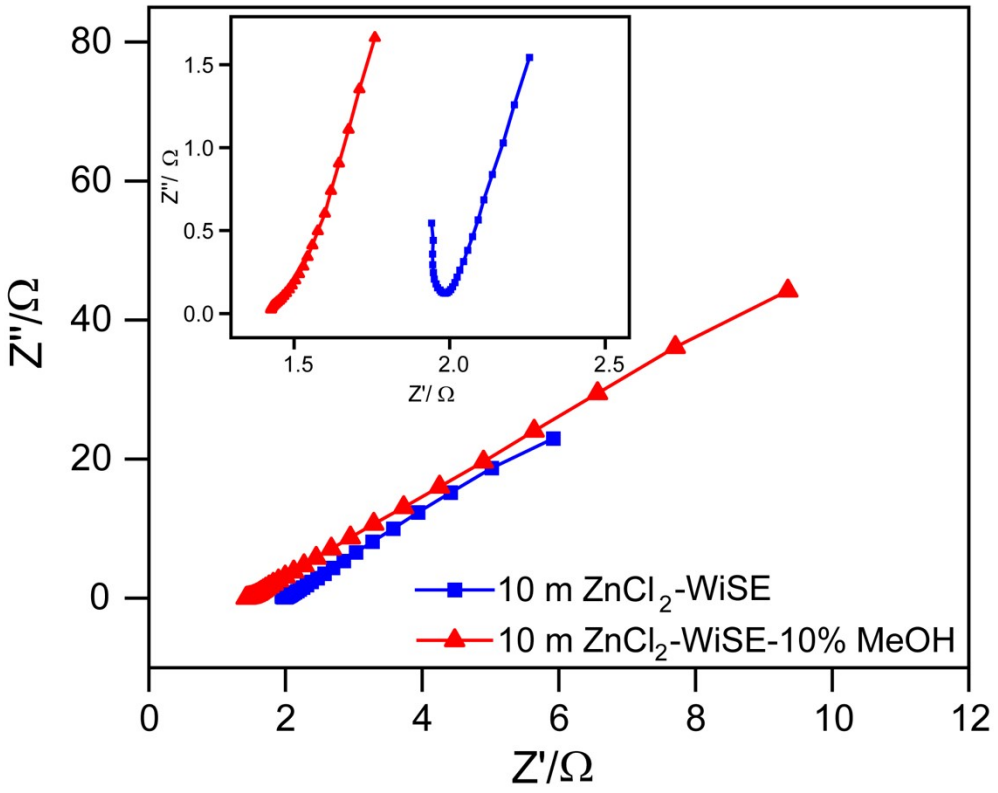

Fig. S10: *Electrochemical impedance spectroscopy (EIS) data of 10 m $ZnCl_2$-WiSE and 10 m $ZnCl_2$-WiSE -10 % MeOH.*

Section S8: Galvanostatic Charge Discharge (GCD) Study

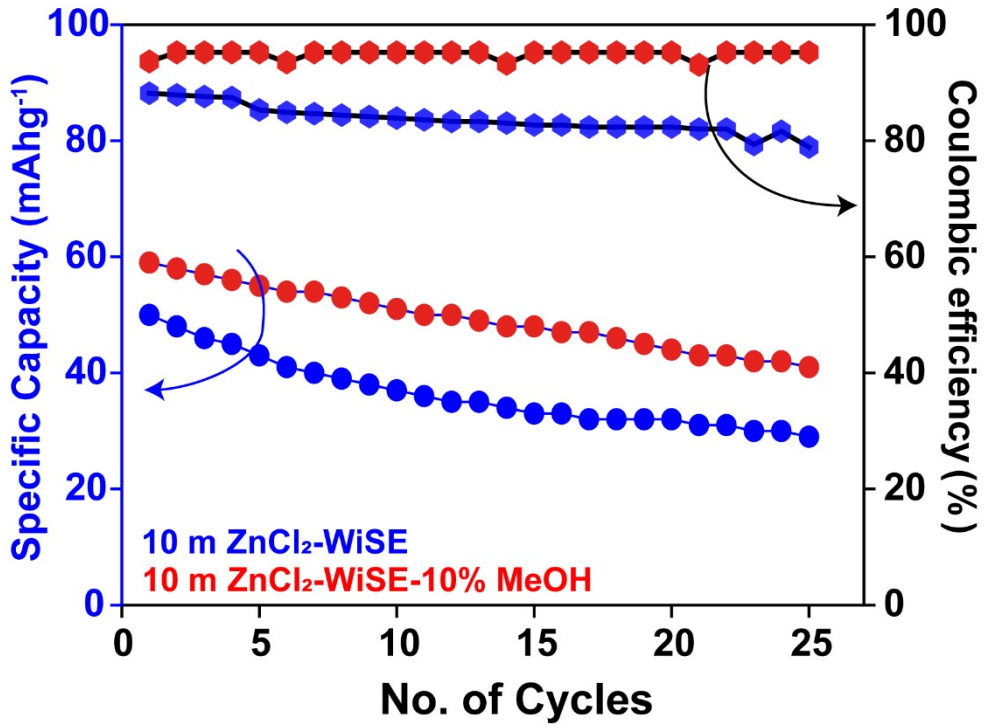

Fig. S11: *Cycling stability of PBAR in 10 m $ZnCl_2$-WiSE and 10 m $ZnCl_2$-WiSE-10% MeOH at 3.3C-rate (1C-rate = 66 mAg^{-1}). Only discharge-specific capacity is shown here.*

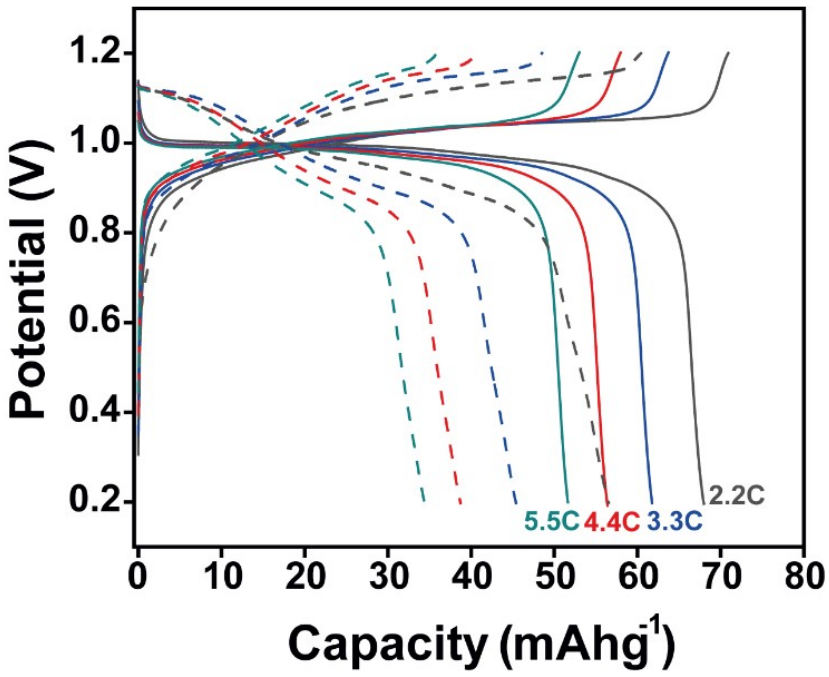

Fig. S12: *Rate capability study comparison of PBAR in 10 m $ZnCl_2$-WiSE (dashed line) and 10 m $ZnCl_2$-WiSE -10% MeOH (solid line) (1C= 66 $mAhg^{-1}$)*

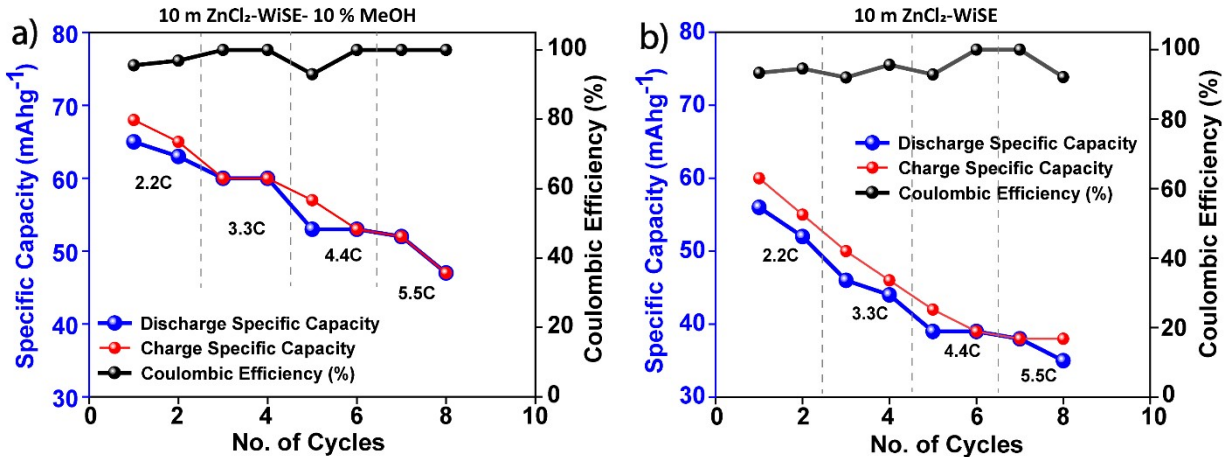

Fig. S13: *Comparison of the rate capability study in 10 m $ZnCl_2$-WiSE and 10 m $ZnCl_2$-WiSE-10% MeOH. (1C=66 $mAhg^{-1}$)*

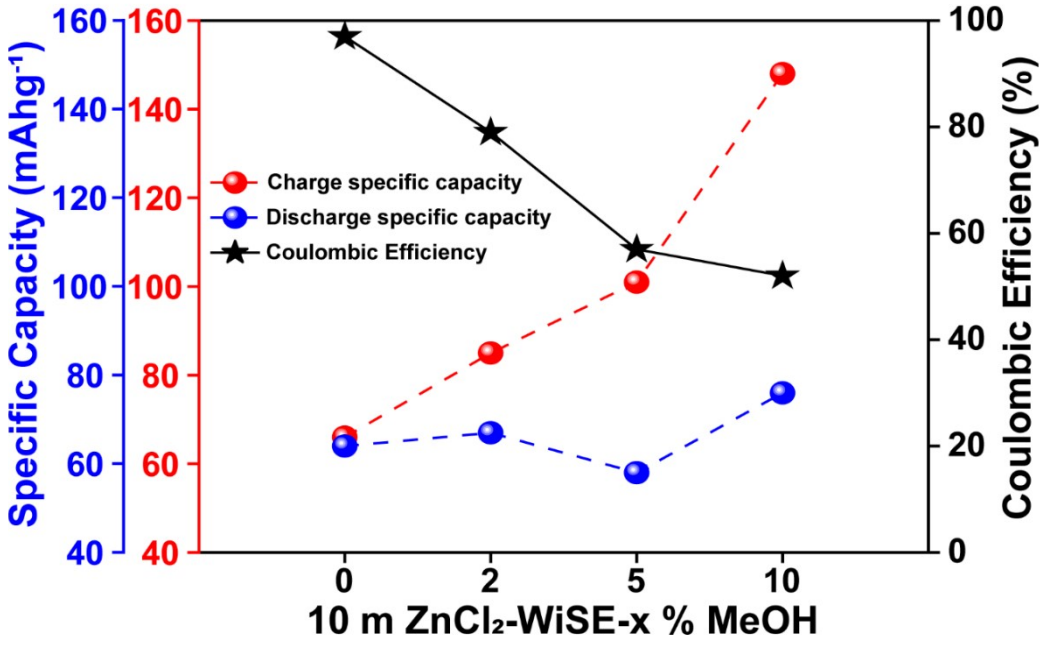

Fig. S14: *Comparison of coulombic efficiency (CE) % of Zn//PBAR full cell, charge-discharge performed at 1C-rate (88 mAg^{-1}) in various concentrations of antisolvent-based electrolyte, 10 m $ZnCl_2$-WiSE-x% MeOH (x=0,2,5,10).*

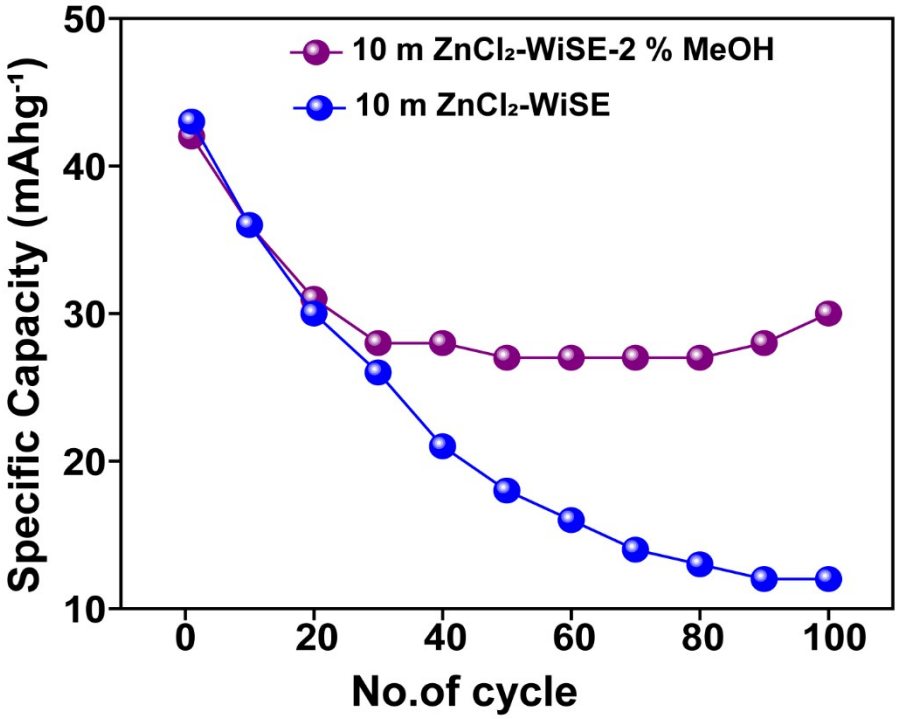

Fig. S15: *Comparison of discharge capacity of cycling study in 10 m $ZnCl_2$-WiSE and 10 m $ZnCl_2$-WiSE-2% MeOH at 6C-rate (1C-rate=88mAg^{-1})*

Section S9: Digital Photograph of Zn-foil after study

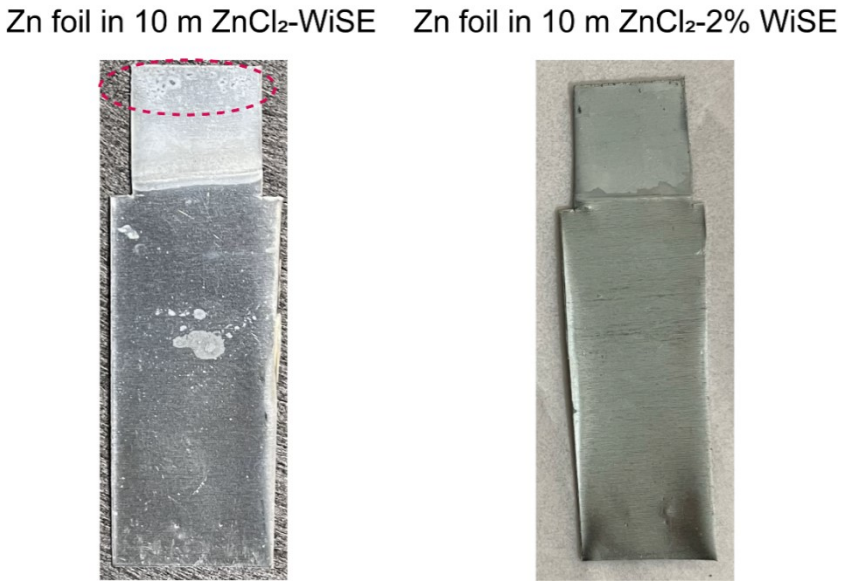

Fig. S16: *Digital photographs of Zn-foil after cycling in 10 m $ZnCl_2$-WiSE (left), and 10 m $ZnCl_2$-WiSE-2% MeOH (right).*

Section S10: SEM images of Zn-foil after study

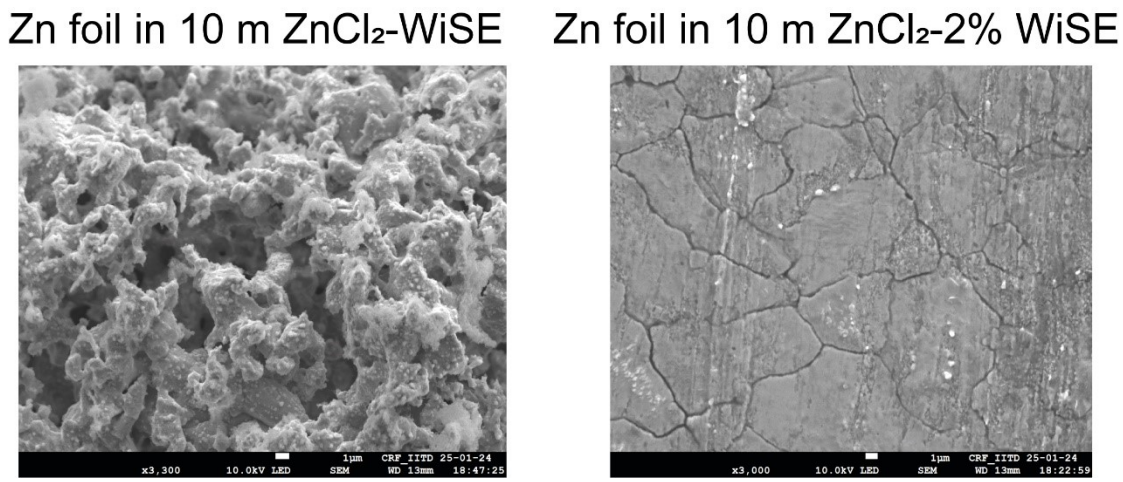

Fig. S17: *Scanning electron microscopy (SEM) images of Zn anode after cycling in 10 m $ZnCl_2$-WiSE (left), and 10 m $ZnCl_2$-WiSE-2% MeOH (right).*

Section S11: Coordination number of different atoms

Table S1: Coordination number of different atoms at the inner solvation shell in 5 m $ZnCl_2$-WiSE-x % MeOH and 10 m $ZnCl_2$-WiSE-x % MeOH, respectively (cutoff distance is shown in parenthesis).

5 m $ZnCl_2$ -x % MeOH	**O_{Water}-O_{Water} (3.3 Å)**	**Zn-O_{Water} (3.6 Å)**	**O_{Water}-O_{MeOH} (3.3 Å)**	**O_{MeOH}-O_{MeOH} (3.3 Å)**
0	4.1	4.6	--	--
5	3.9	4.5	0.07	0.02
10	3.8	4.5	0.15	0.08
15	3.7	4.5	0.21	0.14
10 m $ZnCl_2$ –x % MeOH	**O_{Water}-O_{Water} (3.3 Å)**	**Zn-O_{Water} (3.7 Å)**	**O_{Water}-O_{MeOH} (3.3 Å)**	**O_{MeOH}-O_{MeOH}(3.3 Å)**
0	3.4	3.8	--	--
5	3.3	3.8	0.08	0.02
10	3.2	3.8	0.16	0.07
15	3.1	3.7	0.24	0.15
O_{Water}, O_{MeOH}: oxygen atom of water and methanol molecules respectively.				

Section S12: Diffusion coefficients from MD simulation

Table S2: Diffusion coefficients from MD simulation for Zn^{2+} ions, Cl^- ions, water molecules, and methanol molecules for 5 m $ZnCl_2$-WiSE-x % MeOH and 10 m $ZnCl_2$-WiSE-x % MeOH.

5 m $ZnCl_2$-WiSE-x% MeOH	Diffusion Coefficients (× 10^{-5} cm^2 s^{-1})			
	Zn^{2+} ions	Cl^- ions	Water	Methanol
x = 0	0.1912 ± 0.018	0.3585 ± 0.009	1.0421 ± 0.02	--
x = 5	0.1503 ± 0.009	0.2813 ± 0.008	0.8626 ± 0.02	0.6826 ± 0.15
x = 10	0.1545 ± 0.009	0.2621 ± 0.060	0.8443 ± 0.07	0.5137 ± 0.06
x = 15	0.1497 ± 0.008	0.2594 ± 0.019	0.9140 ± 0.01	0.5953 ± 0.09
10 M $ZnCl_2$ -x% MeOH	**Diffusion Coefficients (× 10^{-6} cm^2 s^{-1})**			
	Zn^{2+} ions	Cl^- ions	Water	Methanol
x = 0	0.0101 ± 0.002	0.0156 ± 0.002	0.2960 ± 0.050	--
x = 5	0.0135 ± 0.001	0.0206 ± 0.005	0.3160 ± 0.003	0.077 ± 0.020
x = 10	0.0149 ± 0.001	0.0311 ± 0.001	0.3940 ± 0.003	0.189 ± 0.010
x = 15	0.0306 ± 0.004	0.0447 ± 0.009	0.5410 ± 0.021	0.243 ± 0.055

Section S13: Efficiency of PBAR in half-cell and Zn//PBAR full-cell

Table S3: Discharge-specific capacity and coulombic efficiency of the PBAR tested in half-cell and full-cell configuration with different methanol vol.% in 10 m $ZnCl_2$-WiSE.

Methanol vol. %	PBAR half-cell @ 1C-rate (1C = 66 mA h g^{-1})	
	Discharge specific capacity (mA h g^{-1})	Coulombic efficiency (%)
0	44	83
10	66	91
15	61	72
Methanol vol. %	**Zn//PBAR Full cell @ 1.3C-rate (1C = 88 mA h g^{-1})**	
	Discharge specific capacity (mA h g^{-1})	Coulombic efficiency (%)
0	64	97
2	67	79
5	58	57
10	76	52